Research Article

Journal of Environmental Nanotechnology

A Comparative Study of PEGylated and PVPylated Surface-functionalized Zinc Oxide Nanoparticles for Environmental Applications

Kuruppanparambil Abdul Rahiman Nisheetha, Sadasivam Narendhran and Madheslu Manikandan*

Department of Bioscience, Sri Krishna Arts and Science College, Kuniamuthur, Coimbatore, TN, India

Received: 26.07.2025 Accepted: 03.09.2025 Published: 30.09.2025

*darwinmani@gmail.com

ABSTRACT

Zinc oxide (ZnO) nanoparticles possess notable antibacterial and photocatalytic properties, yet the lack of comparative studies on PEGylated and PVPylated functionalized ZnO limits understanding of how surface modifications influence their effectiveness. A comparative study was conducted on ZnO nanoparticles synthesized using polyethylene glycol (PEG-ZnO) and polyvinylpyrrolidone (PVP-ZnO) as stabilizing agents, with zinc nitrate as the precursor. The synthesized nanoparticles were characterized using UV–Visible spectroscopy, X-ray diffraction (XRD), energy-dispersive X-ray spectroscopy (EDX), scanning electron microscopy (SEM), and particle size analysis. Antibacterial activity was evaluated against *Escherichia coli* (MTCC: 912), *Bacillus subtilis* (MTCC: 121), and *Streptococcus pyogenes* (MTCC: 1925) using the well diffusion method. Photocatalytic efficiency was assessed through the degradation of methyl orange under sunlight irradiation using 100 mg of catalyst. UV–Vis analysis confirmed the formation of ZnO nanoparticles with absorption peaks at 203 nm (PEG-ZnO) and 207 nm (PVP-ZnO). X-ray diffraction patterns revealed crystalline nature, while EDX analysis confirmed the elemental composition of ZnO. Scanning electron microscopy images showed spherical morphology with minimal aggregation. Particle size analysis indicated average size of 330 ± 80 nm (PEG-ZnO) and 679 ± 45 nm (PVP-ZnO). PEG-ZnO exhibited enhanced antibacterial activity, with inhibition zones of 16.66 ± 0.66 mm (*E. coli*), 16.00 ± 0.88 mm (*B. subtilis*), and 13.66 ± 2.08 mm (*S. pyogenes*) at 100 mg/mL concentration, significantly higher than PVP-ZnO and control ($p < 0.001$). In the degradation study, PEG-ZnO achieved 95.16% methyl orange degradation within 50 minutes, significantly outperforming PVP-ZnO, which showed 84.16% degradation over the same period. These findings suggest that PEG- and PVP-functionalized ZnO nanoparticles are promising candidates for biomedical applications and environmental remediation.

Keywords: Antibacterial activity; Photocatalytic degradation; Polyethylene glycol; Polyvinylpyrrolidone; Zinc oxide nanoparticles; Environmental remediation.

1. INTRODUCTION

Nanotechnology has significantly transformed the development of antibacterial agents by enabling the design of materials with enhanced efficacy and targeted delivery mechanisms. Among various nanomaterials, zinc oxide nanoparticles (ZnO NPs) have gained considerable attention due to their intrinsic antimicrobial properties, biocompatibility, and low cytotoxicity to mammalian cells (Abubakar *et al.* 2022). Their antibacterial activity is primarily attributed to the generation of reactive oxygen species (ROS) upon exposure to light or oxygen, which induce oxidative stress and disrupt bacterial membranes, leading to cell death (Avinash *et al.* 2023). Despite their promising properties, ZnO NPs are prone to aggregation and often require controlled release systems to maintain efficacy and minimize side effects. To address these challenges, encapsulation using biocompatible polymers such as polyvinylpyrrolidone (PVP) and polyethylene glycol (PEG) has been explored (AlAbdulaal *et al.* 2023). These polymers improve the stability, dispersibility, and bioavailability of ZnO NPs, thereby enhancing their antibacterial potential.

In addition to their biomedical utility, ZnO NPs also exhibit photocatalytic activity, which makes them suitable for the degradation of organic pollutants, including toxic dyes in wastewater (Ayub *et al.* 2025). Organic dyes are known to be toxic, persistent, and capable of bioaccumulation, posing risks to aquatic ecosystems and human health (Bhardwaj and Singh, 2023; Endeshaw *et al.* 2025). Moreover, dyes can deplete dissolved oxygen during degradation, creating hypoxic zones and disturbing ecological balance. Their aesthetic impact also compromises water quality and public perception (Gurusamy *et al.* 2024). To address these environmental concerns, various semiconductor metal oxides have been investigated for photocatalytic applications due to their tunable band gaps and high

surface area. For example, Nguyen *et al.* (2025) reported the successful synthesis of ZnO nanoparticles using fruit extracts, which exhibited significant antibacterial and photocatalytic activities under visible light irradiation. Similarly, Nisha *et al.* (2025) demonstrated the eco-friendly fabrication of ZnO nanocomposites using *Lepidium didymium* extract combined with polymer-assisted CTAB/PEG methods, achieving multifunctional properties suitable for biomedical applications. In another study, Panchami *et al.* (2025) developed innovative poly phenylsulfone/silver-doped ZnO membrane systems, highlighting their high-efficiency performance in protein rejection and sustainable separation processes.

Polyvinyl pyrrolidone (PVP) has been widely employed for ZnO NP encapsulation due to its film-forming ability, colloidal stability, and ability to enhance bacterial membrane interactions. Studies by AlAbdulaal *et al.* (2023) and Arshad *et al.* (2020) have demonstrated that incorporating polymers such as PVP, PVA, and PEG in nanomaterial systems significantly enhances structural integrity, optical behavior, and membrane stability. The use of PVPylated nanoparticles, as reported by El-Boubbou *et al.* (2024), contributes to improved dispersibility and biocompatibility, making them effective for biomedical applications like magnetic hyperthermia. Similarly, Khaleel *et al.* (2024) highlighted that PVA-PVP/ZnO nanofibers exhibit favorable morphology, absorption characteristics, and promising antibacterial and anticancer activities, particularly influenced by pH conditions during fabrication.

A comparative assessment by Kumari *et al.* (2025) emphasized that PVP-based hydrogels, synthesized using sterculia gum and zwitterionic sulfobetaine, exhibited excellent biocompatibility and controlled release, supporting their biomedical applicability. Similarly, (Liu *et al.* 2022) demonstrated that $Mg(OH)_2$-loaded PCL/PVP nanofiber membranes showed strong antibacterial properties and biosafety, attributed to the combined effects of PVP polymer matrices and $Mg(OH)_2$ nanoparticles. Additionally, Mezel *et al.* (2024) reported that blending PEG and PVP in fiber coatings enhanced sensor sensitivity and stability, reflecting the broader utility of PEG and PVP as functional stabilizers in nanomaterials, whether for biomedical or sensor applications. Collectively, these findings confirm the capacity of the polymers to improve antibacterial efficacy, biocompatibility, and structural stability of advanced materials. Nazir *et al.* (2021) highlighted the efficient photocatalytic degradation potential of ZnO nanoparticles synthesized using *Eriobotrya japonica* leaves extract, with notable antibacterial activity, underlining the dual-functional application of plant-mediated ZnO nanomaterials. Likewise, Nguyen *et al.* (2025) demonstrated that fruit-extract-mediated ZnO nanoparticles exhibited superior photocatalytic and antibacterial activities, which were attributed to their controlled nanoscale morphology and enhanced surface reactivity. Complementary findings by Prabhu *et al.* (2025) confirmed that ZnO nanoparticles synthesized using *Averrhoa bilimbi* fruit extract achieved effective photocatalytic degradation of dyes, supporting their practical applicability in wastewater treatment. Furthermore, Sheehab *et al.* (2025) demonstrated that TiO_2-SiC nanomaterials integrated into PVA-PEG-based nanocomposites enhanced UV absorption and photocatalytic behavior, reinforcing the relevance of hybrid nanostructures for environmental remediation (Abu *et al.* 2022). Collectively, these studies emphasize the potential of bio-fabricated and composite nanomaterials as efficient photocatalysts for pollutant degradation.

The aim of this study is to systematically compare polyethylene glycol (PEG)-coated (PEGylated) and polyvinylpyrrolidone (PVP)-coated (PVPylated) zinc oxide nanoparticles in terms of their physicochemical properties, antibacterial activity, and photocatalytic degradation efficiency. To achieve this, ZnO nanoparticles were synthesized using a wet chemical precipitation method, followed by surface modification with PEG and PVP. The synthesized nanoparticles were extensively characterized using UV–Visible spectroscopy, Fourier-transform infrared spectroscopy (FTIR), X-ray diffraction (XRD), scanning electron microscopy (SEM), energy-dispersive X-ray spectroscopy (EDX), dynamic light scattering (DLS), and zeta potential analysis to assess their structural, morphological, and surface properties. Further, the antibacterial efficacy of both PEGylated and PVPylated ZnO nanoparticles was evaluated against *Escherichia coli* (MTCC: 912), *Bacillus subtilis* (MTCC: 121), and *Streptococcus pyogenes* (MTCC: 1925) using standard microbial assays to determine their potential as antibacterial agents. Photocatalytic activity was assessed by monitoring the degradation of methyl orange dye under direct sunlight. Finally, the results were compared to analyze the influence of PEG and PVP surface modifications on the stability, antibacterial potential, and photocatalytic performance of ZnO nanoparticles. This comparative evaluation aims to provide deeper understandings into how polymeric surface coatings enhance the multifunctional capabilities of ZnO nanoparticles, contributing to their potential applications in environmental remediation and biomedical fields.

2. MATERIALS AND METHODS

2.1 Materials

Zinc nitrate hexahydrate ($Zn(NO_3)_2 \cdot 6H_2O$), polyethylene glycol (PEG, MW ~4000), and polyvinylpyrrolidone (PVP, MW ~10,000) were procured from HiMedia Laboratories (Mumbai, India). Methyl orange dye was obtained from Merck (India). All

chemicals used were of analytical grade and utilized without further purification. Deionized water was used throughout the experiments. Bacterial strains *Escherichia coli* (MTCC 912), *Bacillus* subtilis (MTCC 121), and *Streptococcus pyogenes* (MTCC 1925) were acquired from the Microbial Type Culture Collection (MTCC), Chandigarh, India.

2.2 Synthesis of ZnO Nanoparticles with PEG and PVP

Zinc oxide nanoparticles were synthesized using PEG and PVP as stabilizing and capping agents *via* a wet chemical precipitation method (Magar *et al.* 2022; Raha *et al.* 2022). For each synthesis, 100 mL of distilled water was heated to 80°C in a water bath. One gram of the respective polymer (PEG or PVP) was added to the heated water and stirred continuously until a homogeneous dispersion was achieved. A 0.1 M aqueous solution of $Zn(NO_3)_2 \cdot 6H_2O$ was prepared and gradually introduced into the polymer solution under constant magnetic stirring. Upon achieving a uniformly mixed solution, 4 g of NaOH pre-dissolved in 50 mL of distilled water was added dropwise. This step facilitated the nucleation and growth of zinc oxide nanoparticles, evidenced by the appearance of a milky white suspension. The mixture was left undisturbed at room temperature until complete precipitation occurred, resulting in a white solid settling at the bottom and a clear supernatant on top. The precipitate was collected by centrifugation, washed three times with distilled water to remove unreacted precursors, followed by two washes with 70% ethanol to eliminate organic residues. The cleaned nanoparticle pellet was dried in a crucible at 80°C for 8 hours in a hot air oven. After drying, the aggregated mass was finely ground using a sterile mortar and pestle to obtain a uniform nanoparticle powder. The resulting PEG-ZnO and PVP-ZnO nanopowders were labeled and stored in airtight containers for further characterization and application studies.

2.3 Characterization of PEG-ZnO and PVP-ZnO Nanoparticles

The optical properties of the nanoparticles were analyzed using a UV–Visible spectrophotometer (Shimadzu UV-2600) in the range 200–800 nm. Crystallographic patterns were recorded using an X-ray diffractometer (Bruker D8 Advance) with Cu-Kα radiation (λ = 1.5406 Å) at a scanning rate of 2°/min in the 2θ range 10°–80°. Elemental composition was examined using an EDX system (JEOL JSM-7610F). Morphological features were analyzed using SEM to observe particle shape and surface texture. Dynamic light scattering (DLS) was employed using a Malvern Zetasizer Nano ZS to determine the hydrodynamic diameter of the nanoparticles.

2.4 Antibacterial Activity of PEG-ZnO and PVP-ZnO Nanoparticles

The antibacterial activity of PEG- and PVP-mediated zinc oxide nanoparticles was assessed using the agar well diffusion method against *Escherichia coli* (MTCC 912), *Bacillus subtilis* (MTCC 121), and *Streptococcus pyogenes* (MTCC 1925) (Uzoeto *et al.* 2024). Each bacterial strain was cultured in nutrient broth for 18–24 hours at 37°C, and the inoculum was adjusted to approximately 10^6 CFU/mL using McFarland standard. Sterile nutrient agar plates were prepared and uniformly swabbed with 100 µL of the standardized bacterial suspension using a sterile cotton swab. Wells of 6 mm diameter were punched aseptically into the agar using a sterile gel borer. Into each well, 50 µL of PEG-ZnO or PVP-ZnO nanoparticle suspensions at different concentrations (25, 50, 75, and 100 mg/mL) were added. Streptomycin (10 µg/mL) was used as a positive control, and sterile distilled water served as the negative control. The plates were incubated at 37°C for 24 hours. After incubation, the zones of inhibition were measured in millimeters. All experiments were performed in triplicate, and results were reported as mean ± standard deviation (SD). Statistical significance was determined using one-way ANOVA, with $p < 0.05$ considered significant.

2.5 Photocatalytic Degradation of Methyl Orangeusing PEG-ZnO and PVP-ZnO Nanoparticles

The photocatalytic degradation of methyl orange (MO) was carried out using PEGylated and PVPylated zinc oxide nanoparticles under natural sunlight (Villegas *et al.* 2024). A 100 mL aqueous solution of MO was prepared at a concentration of 10 mg/L, to which 100 mg of either PEG-ZnO or PVP-ZnO nanoparticles were added. The suspension was stirred in the dark for 30 minutes to establish adsorption–desorption equilibrium between the dye molecules and nanoparticle surfaces. Following this, the mixture was exposed to direct natural sunlight with continuous stirring to initiate photocatalytic degradation. At regular intervals, 5 mL aliquots were withdrawn from the suspension, centrifuged at 10,000 rpm to separate the nanoparticles, and the clear supernatant was analyzed using UV–Visible spectrophotometry at 464 nm to monitor the degradation of MO. The degradation efficiency (%) was calculated using the formula:

$$Degradation\ efficiency\ \% = \left(\frac{Co-Ct}{Co}\right) \times 100 \ldots (1)$$

where C_0 represents the initial absorbance of MO, and C_t is the absorbance at time t.

The first-order kinetic formula has measured the rate constant

$$\ln\left(\frac{C}{C_o}\right) = -kt \quad \ldots (2)$$

The term C, Co refers to the initial and final concentration of dye, where k denotes rate constant, and t indicates the time. All experiments were performed in triplicate to ensure reproducibility, and the photocatalytic efficiencies of PEG-ZnO and PVP-ZnO nanoparticles were compared based on their degradation performance.

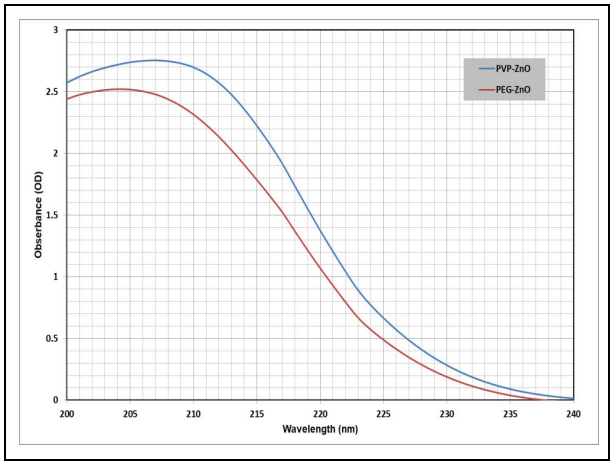


Fig. 1: The UV-vis analysis of PVP-ZnO and PEG-ZnO shows broad peaks at 203 nm and 207 nm, respectively

3. RESULTS AND DISCUSSION

3.1 UV-vis

The UV-Vis absorption spectra of PVP-ZnO and PEG-ZnO are shown in Fig. 1. Both PVP-ZnO and PEG-ZnO exhibit strong optical absorbance peaks at 203 nm and 207 nm, respectively. According to Arshad *et al.* (2020), the incorporation of polymers such as PVP in composite materials enhances optical clarity and stability due to effective polymer–nanoparticle interactions, which may explain the distinct absorption observed for PVP-ZnO. Similarly, Coll *et al.* (2024) demonstrated that PEG-mediated encapsulation strategies improve the structural and functional properties of nanomaterials, contributing to their well-defined optical responses, as reflected in the PEG-ZnO absorption peak at 207 nm. Furthermore, El-Boubbou *et al.* (2024) reported that PVP coating enhances nanoparticle surface functionality and dispersion in aqueous media, factors that likely contribute to the pronounced UV absorption behavior of PVP-ZnO nanoparticles in this study. The slight difference in absorption peaks between PVP-ZnO and PEG-ZnO could be attributed to variations in polymer–ZnO interactions and the degree of surface modification, affecting the electronic transitions within the nanoparticles. The observed UV–Vis spectra confirm successful polymer functionalization and nanoscale integrity of both PVPylated and PEGylated ZnO nanoparticles.

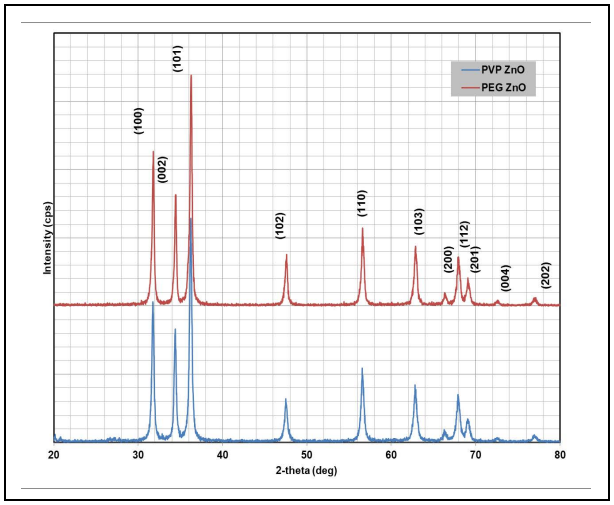


Fig. 2: XRD analysis of PEG-ZnO and PVP-ZnO nanoparticles

3.2 XRD Analysis of PEG-ZnO and PVP-ZnO Nanoparticles

The XRD analysis of both PVP-coated and PEG-coated ZnO nanoparticles confirmed their hexagonal wurtzite crystalline structure (Fig. 2). In both samples, the most intense diffraction peak was recorded at $2\theta = 36.3°$, corresponding to the (101) plane, indicative of well-defined crystallinity. Additional peaks were identified at $2\theta = 31.8°$ (100), 47.6° (102), and 66.3° (110), matching standard ZnO diffraction patterns. The calculated lattice parameters for both samples were $a = 0.325$ nm and $c = 0.520$ nm, derived using the Bragg equation, confirming the structural consistency of ZnO after polymer coating. These findings indicate that surface functionalization with PVP and PEG did not significantly alter the crystal structure of ZnO but preserved its nanoscale crystallinity.

The XRD patterns confirm the formation of crystalline ZnO nanoparticles with a wurtzite hexagonal structure, similar to a reported work (Kaur *et al.* 2025). The presence of sharp and well-defined peaks indicates high crystallinity, a crucial factor for photocatalytic performance. The retention of the wurtzite structure after PEG and PVP surface modification suggests that the polymer coating did not disrupt the intrinsic crystal lattice of ZnO. The calculated lattice parameters are consistent with standard ZnO values, reaffirming structural stability post-polymer functionalization. Similar trends were observed by Khaleel *et al.* (2024) in PVA-PVP/ZnO nanofibers, where polymer incorporation preserved the ZnO crystalline phase. Jailani *et al.* (2025) demonstrated that polymer-assisted ZnO composites retain nanoscale crystallinity while benefiting from enhanced dispersion and stability. The XRD results validate that PEG and PVP coatings effectively stabilize ZnO nanoparticles without compromising their structural integrity or crystallinity, aligning with prior reports on

polymer-stabilized metal oxide nanomaterials (Kaur *et al.* 2025).

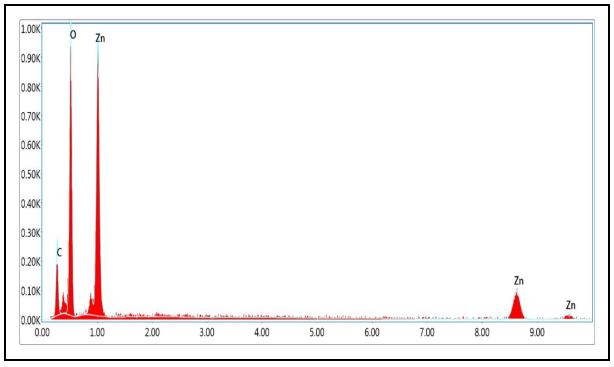


Fig. 3: EDX images of synthesized PEG – ZnO nanoparticles

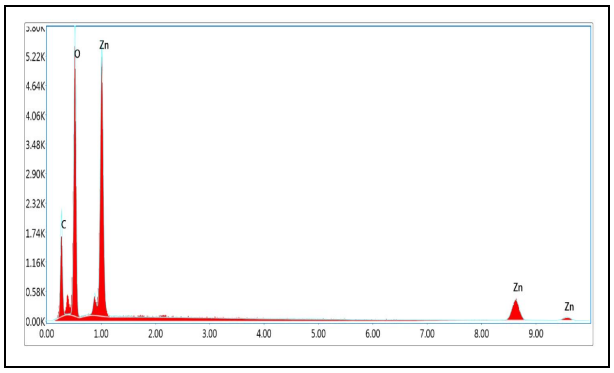


Fig. 4: EDX images of synthesized PVP – ZnO nanoparticles

3.3 EDX Analysis of ZnO Nanoparticles

The EDX analysis reveals the elemental composition of PVP-ZnO and PEG-ZnO nanoparticles, highlighting the presence of zinc (Zn) and oxygen (O) as the primary constituents (Fig. 3 & Fig. 4). In the case of PEG-ZnO nanoparticles, Zn accounts for approximately 54.69% of the total weight and 20.95% of the atomic composition, while O comprises about 29.64% of the weight and 46.38% of the atomic composition (Table 1). These results indicate a relatively higher concentration of zinc compared to oxygen, suggesting a higher density of zinc atoms within the nanoparticle structure.

Conversely, for PVP-ZnO nanoparticles, Zn constitutes approximately 45.32% of the total weight and 15.21% of the atomic composition, while O makes up about 33.19% of the weight and 45.52% of the atomic composition. Here, the weight percentages of zinc and oxygen are more comparable, indicating a more balanced elemental composition compared to PEG-ZnO nanoparticles. The differences in elemental composition between PEG-ZnO and PVP-ZnO nanoparticles can be attributed to the nature of the polymer coatings (polyethylene glycol for PEG-ZnO and polyvinylpyrrolidone for PVP-ZnO). These polymers may interact differently with the surface of the zinc oxide nanoparticles, influencing the distribution and concentration of zinc and oxygen atoms within the nanocomposite structure (Sharma *et al.* 2023).

3.4 SEM and Elemental Overlay Image

The scanning electron microscopy (SEM) images of zinc oxide nanoparticles are depicted in Fig. 5 and Fig. 6. The analysis of these images reveals distinct characteristics regarding the morphology and distribution of the nanoparticles. From the SEM images, it is evident that the zinc oxide nanoparticles exhibit a spherical shape and are well distributed throughout the sample. However, some degree of aggregation is observed, indicating a tendency for particle clustering. This aggregation phenomenon is common in nanoparticle systems and can be influenced by factors such as synthesis conditions and surface chemistry. Moreover, elemental analysis through EDX provides insights into the elemental composition of the zinc oxide nanoparticles. The elemental overlay images depict the relative abundance of Zn, O, and C within the nanoparticles. For the PEG-coated zinc oxide nanoparticles, the elemental overlay image indicates the presence of approximately 20% zinc, 67% oxygen, and 13% carbon. Conversely, the elemental composition of the PVP-coated zinc oxide nanoparticles reveals approximately 14% zinc, 67% oxygen, and 19% carbon.

These elemental compositions reflect the influence of the polymer coating on the surface chemistry of the zinc oxide nanoparticles. The differences in carbon content suggest variations in the degree of polymer coverage and the nature of interactions between the polymer matrix and the nanoparticle surface. Additionally, the consistent oxygen content in both samples indicates the predominant presence of zinc oxide as the primary constituent.

3.5 Particle Size Analysis of ZnO Nanoparticles

The particle size analysis provides insights into the size distribution and average sizes of PVP-ZnO and PEG-ZnO nanoparticles (Fig. 7 & Fig. 8). For PEG-ZnO nanoparticles, the size distribution peaks at approximately 232 nm, with a Z-average particle size of 330 ± 80 nm. The polydispersity index (PdI) of PEG-ZnO nanoparticles is calculated to be 0.632, indicating a relatively narrow size distribution and moderate particle uniformity. In contrast, PVP-ZnO nanoparticles exhibit a size distribution peak at around 302 nm, with a significantly larger Z-average size of 679 ± 45 nm. The PdI value of 1.000 for PVP-ZnO nanoparticles suggests a broader size distribution and greater particle heterogeneity compared to PEG-ZnO nanoparticles (Table 2). These variations in nanoparticle size and dispersity may be attributed to differences in synthesis conditions, surface coatings, and stabilization mechanisms provided by polyvinylpyrrolidone (PVP) and polyethylene glycol (PEG) (Lin *et al.* 2024).

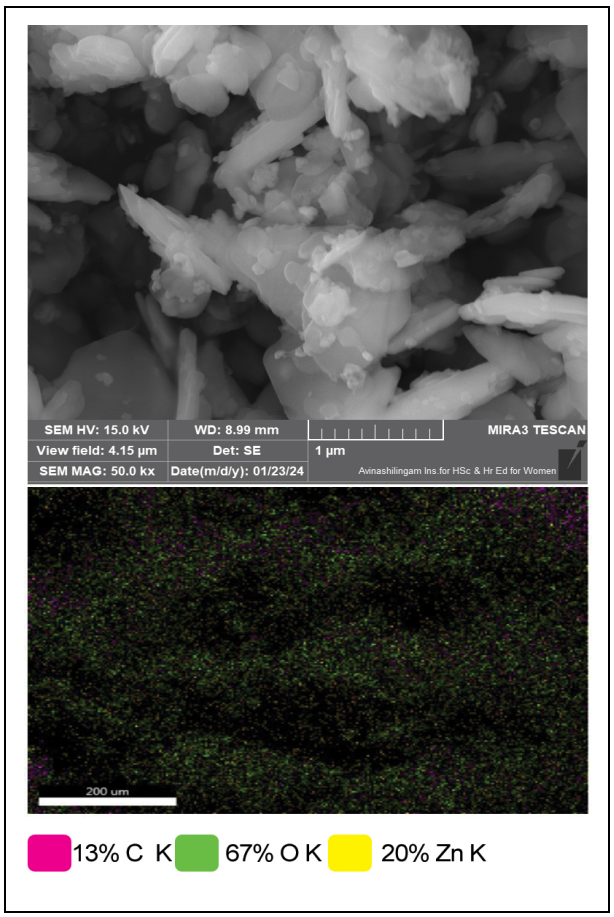


Fig. 5 (a&b): SEM and elemental overlay images of synthesized PEG ZnO nanoparticles

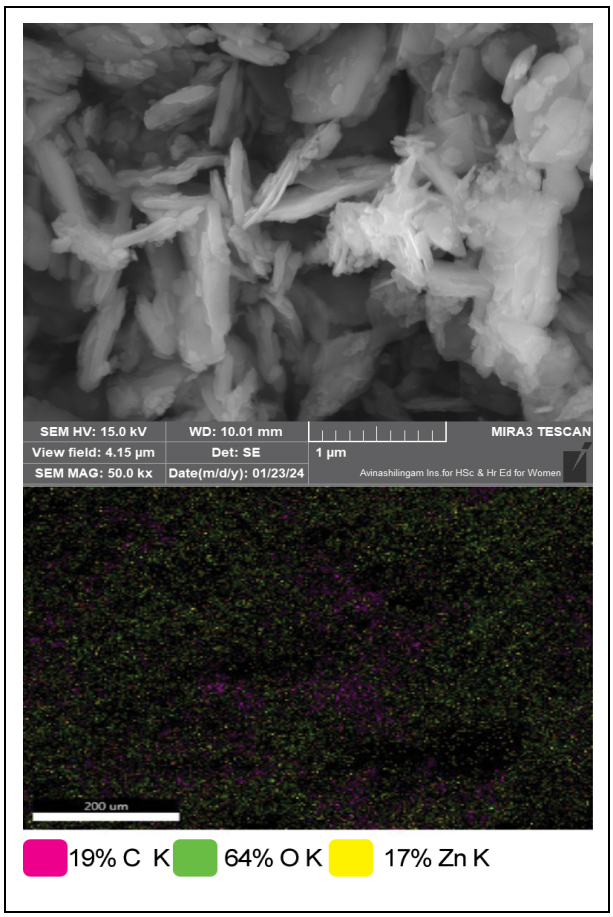


Fig. 6 (a&b): SEM and elemental overlay images of synthesized PEG ZnO nanoparticles

Table 1. Elemental composition of ZnO nanoparticles using PEG and PVP

Nanoparticles	Element	Weight (%)	Atomic (%)
PEG-ZnO	Zn	54.69	20.95
	O	29.64	46.38
PVP-ZnO	Zn	45.32	15.21
	O	33.19	45.52

Table 2. The average size distribution of PVP-ZnO and PEG-ZnO NMs estimated by using particle size analysis

Nanoparticles	Size Distribution (d.nm)	Z-Average Size (d.nm)	Width (d.nm)	PdI
PEG-ZnO	232	330	80.12	0.632
PVP-ZnO	302	679	45.41	1.000

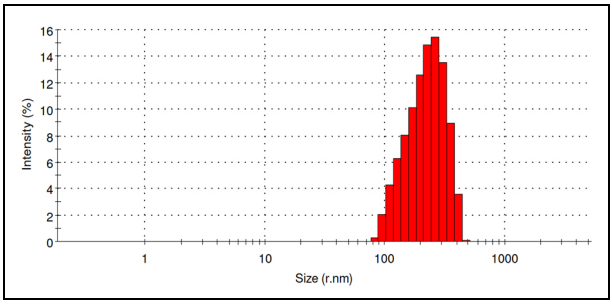


Fig. 7: DLS analysis of PEG-ZnO nanoparticles

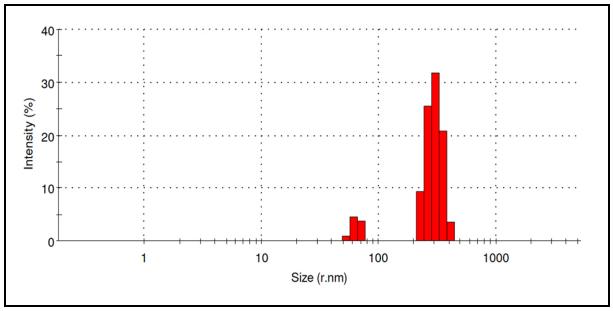


Fig. 8: DLS analysis of PVP-ZnO nanoparticles

3.6 Antibacterial Activity of Zinc Oxide Nanoparticles

The PEG- and PVP-mediated zinc oxide nanoparticles show an excellent antibacterial activity against bacterial pathogenic. Highest zone of inhibition was observed in PEG-ZnO NPs against *E. coli* with a zone of inhibition diameter of 16.66 ± 0.66 mm at a concentration 100 mg/mL and lowest inhibition in *Streptococcus pyrogenes* with zone diameter 13.66 ± 2.08 mm at same concentration (Table 3). PEG-mediated zinc oxide nanoparticles showed effective antibacterial activity in *E. coli*. Likewise, PVP-ZnO nanoparticles show maximum zone of inhibition observed in *E. coli* (15.16 ± 0.44 mm) and minimum zone of inhibition in *Streptococcus pyrogenes* (13.83 ± 0.92 mm) at the concentration of 100 mg/mL (Table 4).

Rutherford *et al.* (2025) evaluated the antibacterial efficacy of PEG-encapsulated ZnO nanoparticles against *Pseudomonas aeruginosa*. They reported a zone of inhibition with a diameter of 17.3 ± 0.5 mm at a concentration of 100 mg/mL. PEGylation enhanced the stability of ZnO NPs and facilitated sustained release, leading to effective bacterial membrane disruption and oxidative stress induction, as evidenced by TEM and ROS assays. Khaleel *et al.* (2024) investigated the antibacterial properties of PVP-encapsulated ZnO nanofibers against *Staphylococcus aureus*. They observed a zone of inhibition with a diameter of 15.8 ± 0.6 mm at 100 mg/ml. PVP coating improved the dispersibility and stability of ZnO NPs, ensuring sustained antibacterial effects through enhanced membrane interactions and ROS-mediated bacterial cell damage. Sheehab *et al.* (2025) compared the antibacterial activities of PEG and PVAencapsulated TiO_2-SiC nanomaterials against *Salmonella typhi* and *Streptococcus pneumoniae*. They found that PEG/TiO_2-SiC NPs exhibited a larger zone of inhibition against both bacterial strains compared to PVA/ TiO_2-SiC NPs, with statistical significance ($p < 0.05$). This study highlighted the superior antibacterial efficacy of PEGylation due to enhanced nanoparticle stability and prolonged release kinetics.

Ayub *et al.* (2025) investigated the antibacterial efficacy of polyethylene glycol (PEG)-encapsulated zinc oxide nanoparticles (ZnO NPs) against *Escherichia coli* and *Staphylococcus aureus*. They reported significant zones of inhibition with diameters of 16.5 ± 0.3 mm and 14.8 ± 0.5 mm, respectively, at a concentration of 100 mg/ml. Babaei *et al.* (2023) synthesized and assessed polyvinylpyrrolidone (PVP)-encapsulated ZnO NPs for their antibacterial activity against *Pseudomonas aeruginosa*, observing a zone of inhibition with a diameter of 15.2 ± 0.4 mm at 100 mg/mL. De-Lucas *et al.* (2018) conducted a comparative study on the antibacterial activities of PEG- and PVP-encapsulated ZnO NPs against *Streptococcus pneumoniae* and *Acinetobacter baumannii*, revealing that PEG-ZnO NPs exhibited larger zones of inhibition against both bacterial strains compared to PVP-ZnO NPs, with statistical significance ($p < 0.05$). Nisha *et al.* (2025) evaluated the antibacterial efficacy of CTAB/PEG-encapsulated ZnO NPs against *E. coli* and *S. aureus*, reporting zones of inhibition with diameters of 15.7 ± 0.6 mm and 14.5 ± 0.4 mm, respectively, at 100 mg/mL. Ahmad and Kalra (2020) synthesized ZnO NPs and assessed their antibacterial activity against *P. aeruginosa*, noting a zone of inhibition with a diameter of 14.9 ± 0.3 mm at 100 mg/mL. This collective evidence highlights the superior antibacterial efficacy of PEGylation, attributed to enhanced nanoparticle stability and sustained release kinetics.

Table 3. Antibacterial activity of PVP-ZnO nanoparticles against bacteria pathogen. The resulted zone of inhibition (mm) are expressed in Mean ± SE

Pathogens	Different concentration of PVP-ZnO Nanoparticles				Control (Streptomycin 10 µg/mL)
	25 mg/mL	50 mg/mL	75 mg/mL	100 mg/mL	
E. coli	12.00 ± 1.15	12.00 ± 0.57	13.00 ± 0.57	16.66 ± 0.66	14.66 ± 1.85
B. subtilis	13.00 ± 0.57	13.33 ± 0.88	14.00 ± 1.00	16.00 ± 0.88	16.16 ± 0.44
S. pyogenes	15.16 ± 0.76	15.00 ± 2.00	15.66 ± 1.52	13.66 ± 2.08	17.16 ± 0.44

Table 4. Antibacterial activity of PEG-ZnO nanoparticles against bacteria pathogen. The resulted zone of inhibition (mm) are expressed in Mean ± SE

Pathogens	Different concentration of PEG-ZnO Nanoparticles				Control (Streptomycin 10 µg/mL)
	25 mg/mL	50 mg/mL	75 mg/mL	100 mg/mL	
E. coli	12.83 ± 0.44	13.00 ± 0.28	13.50 ± 0.28	15.16 ± 0.44	12.83 ± 0.44
B. subtilis	12.50 ± 0.28	12.00 ± 0.57	14.00 ± 1.52	13.00 ± 0.57	14.83 ± 0.44
S. pyogenes	13.16 ± 0.60	12.33 ± 0.33	10.50 ± 0.28	13.83 ± 0.92	12.62 ± 0.44

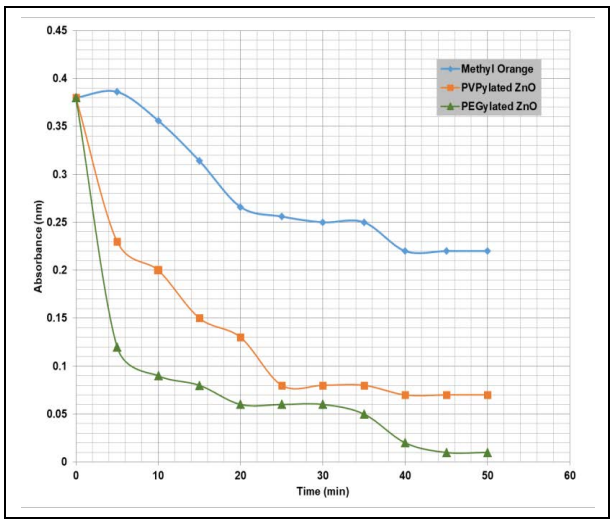


Fig. 9: Photocatalytic degradation of methyl orange (MO) under sunlight using PEGylated ZnO and PVPylated ZnO nanoparticles, showing absorbance reduction over time

3.7 Photocatalytic Activity of ZnO Nanoparticles

The photocatalytic degradation results demonstrated that both PEGylated ZnO and PVPylated ZnO nanoparticles effectively facilitated methyl orange (MO) dye degradation under sunlight, with PEG-ZnO exhibiting superior performance. As indicated in Fig. 9 and Fig. 10, PEG-ZnO achieved over 95% degradation within 50 minutes, while PVP-ZnO reached approximately 85% degradation in the same duration. The enhanced degradation efficiency of PEG-ZnO can be attributed to its smaller particle size and improved dispersibility, which likely increased the surface-active sites for photocatalytic reactions, as supported by Ayub *et al.* (2025) and Nisha *et al.* (2025), who emphasized the role of PEG in stabilizing metal oxide nanostructures and promoting charge separation.

The kinetic analysis (Fig. 11) further confirmed this trend, with PEG-ZnO displaying a higher correlation coefficient ($R^2 = 0.9362$) and a lower rate constant value than PVP-ZnO ($R^2 = 0.8055$), indicating more consistent photocatalyticbehavior. Bhardwaj and Singh, (2023), reported that polymer-assisted ZnO nanomaterials showed efficient dye degradation due to minimized aggregation and optimized electron–hole generation. The superior performance of PEG-ZnO aligns with the structural advantages reported by AlAbdulaal *et al.* (2023) and Sheehab *et al.* (2025), highlighting the role of polymer matrices like PEG in enhancing nanomaterial morphology and catalytic activity through improved light absorption and reactive oxygen species (ROS) generation. In contrast, the relatively lower degradation efficiency of PVP-ZnO, though still significant, might be due to its larger particle size and broader size distribution, potentially limiting active surface exposure, as observed by El-Boubbou *et al.* (2024) and Khaleel *et al.* (2024). The present study highlights that PEG-functionalized ZnO nanoparticles outperform PVP-coated ZnO in sunlight-driven photocatalytic degradation of MO dye. Both the catalysts are effective and sustainable photocatalysts for environmental remediation applications.

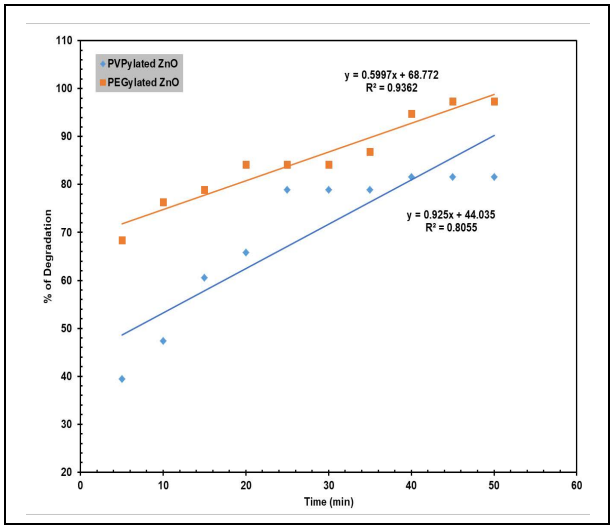


Fig. 10: Percentage degradation of methyl orange dye over time by PEG-ZnO and PVP-ZnO nanoparticles, indicating higher degradation efficiency of PEG-ZnO

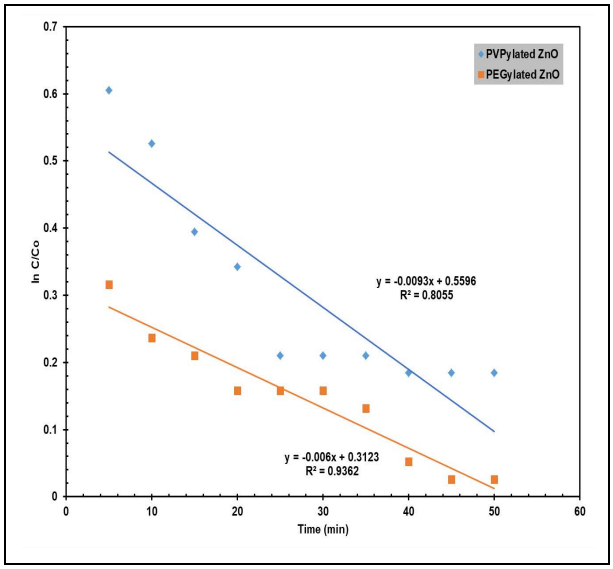


Fig. 11: Pseudo-first-order kinetic plots for methyl orange degradation using PEG-ZnO and PVP-ZnO nanoparticles, illustrating rate constants and correlation coefficients (R^2)

4. CONCLUSION

The present study systematically compared PEGylated and PVPylated zinc oxide (ZnO) nanoparticles in terms of their physicochemical characteristics, antibacterial efficacy, and photocatalytic performance. Both nanoparticle systems were successfully synthesized using zinc nitrate as a precursor, with PEG and PVP serving as stabilizing and surface-

modifying agents. Structural analysis *via* XRD confirmed the hexagonal wurtzite crystal phase for both PEG-ZnO and PVP-ZnO nanoparticles, with prominent diffraction peaks corresponding to the (100), (002), (101), and (110) planes, indicating high crystallinity. Morphological examination using SEM revealed that both nanoparticle types exhibited predominantly spherical morphology, with minimal aggregation, suggesting effective surface stabilization by both polymers. Elemental composition, confirmed through EDX confirmed the presence of zinc and oxygen as principal components, with no significant impurities detected.

Dynamic light scattering (DLS) analysis provided insights into the hydrodynamic particle size distribution. PEG-ZnO nanoparticles exhibited a smaller average size of 330 ± 80 nm and a polydispersity index (PdI) of 0.632, indicating moderate uniformity. Conversely, PVP-ZnO nanoparticles showed a larger average size of 679 ± 45 nm with a PdI of 1.000, suggesting broader size distribution and greater particle heterogeneity. Additionally, PEG-ZnO exhibited stronger antibacterial activity against *E. coli*, *B. subtilis*, and *S. pyogenes*, attributed to its smaller size and higher surface reactivity. Functionally, PEGylated ZnO nanoparticles demonstrated superior photocatalytic degradation efficiency against methyl orange dye, achieving over 95% degradation under sunlight irradiation within 50 minutes, outperforming PVP-ZnO. The findings establish that PEGylation confers better control over nanoparticle size, improved dispersibility, and enhanced functional performance compared to PVPylation. Therefore, PEG-ZnO nanoparticles are recommended as a promising candidate for environmental remediation and biomedical applications, particularly in antibacterial coatings and photocatalytic wastewater treatment.

ACKNOWLEDGMENT

We acknowledge the management of Sri Krishna Arts and Science College, Coimbatore, TN India for providing necessary facilities to carry out this study.

AUTHOR CONTRIBUTIONS

Kuruppanparambil Abdul Rahiman Nisheetha - Implementation of Experimental design. Madheslu Manikandan - Planning and Supervision of experimental design, Data analysis and Result interpretation. Sadasivam Narendhran - Data analysis and Result interpretation, Manuscript preparation.

FUNDING

This research received no specific grant from any funding agency in the public, commercial, or not-for-profit sectors.

CONFLICTS OF INTEREST

The authors declare that there is no conflict of interest.

COPYRIGHT

This article is an open-access article distributed under the terms and conditions of the Creative Commons Attribution (CC BY) license (http://creativecommons.org/licenses/by/4.0/).

REFERENCES

Abu, N. S. M., Shah, S. S., Chaity, S. B., Biswas, B. K., Nahar, B., Aziz, M. A. and Hossain, M. Z., Jute stick extract assisted hydrothermal synthesis of zinc oxide nanoflakes and their enhanced photocatalytic and antibacterial efficacy, *Arabian J. Chem*., 15(11), 104265(2022). https://doi.org/10.1016/J.ARABJC.2022.104265

Abubakar, H. L., Tijani, J. O., Abdulkareem, S. A., Mann, A. and Mustapha, S., A review on the applications of zinc tungstate ($ZnWO_4$) photocatalyst for wastewater treatment, *Heliyon*, 8(7), e09964(2022). https://doi.org/10.1016/J.HELIYON.2022.E09964

Ahmad, W. and Kalra, D., Green synthesis, characterization and antimicrobial activities of ZnO nanoparticles using Euphorbia hirta leaf extract, *J. King Saud Univ. Sci.,* 32(4), 2358–2364(2020). https://doi.org/10.1016/j.jksus.2020.03.014

AlAbdulaal, T. H., Abdullah, W. and Yahia, I. S., Synthesizing and exploring the structural and optical properties of PVA/PVP/PEG polymeric sheet upon doping with nano nickel oxide (NiO) for CUT-OFF filters, *J. Mater. Res. Technol*., 27, 8308–8322(2023). https://doi.org/10.1016/J.JMRT.2023.11.199

Arshad, M., Neelam, A., Haleem, N., Jamal, Y., Hina, K., Bilal, M., Shah, S. H., Hussain, I. and Zhang, Y., Synthesis and characterization of CMC/PVA/PVP composite microfiltration membrane, *Desalin. Water Treat.*, 203, 70–79(2020). https://doi.org/10.5004/DWT.2020.26227

Avinash, B., Ravikumar, C. R., Basavaraju, N., Abebe, B., Kumar, T. N., Manjula, S. N. and Murthy, H. C. A., Facile green synthesis of zinc oxide nanoparticles: Its photocatalytic and electrochemical sensor for the determination of paracetamol and D-glucose, *Environ. Func. Mater*., 2(2), 13–141(2023). https://doi.org/10.1016/J.EFMAT.2024.01.002

Ayub, Y., Farrukh, M. A., Ben, K. S., Chebaane, S., Ghodhbani, R., Ismail, M. A., Ibrar, M., Munawar, T. and Allakhverdiev, S. I., In-situ synthesis of polyethylene glycol-assisted combined semiconductor metallic oxides nanocomposite for solar cell, supercapacitor, photocatalytic, and antibacterial applications, *Ceram. Int.,* 51(23), 28342(2025). https://doi.org/10.1016/J.CERAMINT.2025.06.177

Babaei, P., Safaei, G. J., Rashki, S. and Mahmoudi, K. A., Morphology modified by polyvinylpyrrolidone for enhanced antibacterial and catalytic execution of bioactive Ag/ZnO composites based on hydroxyapatite in the synthesis of O-Aminocarbonitriles, *Ceram. Int*., 49(14), 22826–22836(2023). https://doi.org/10.1016/J.CERAMINT.2023.04.106

Bhardwaj, K. and Singh, A. K., Bio-waste and natural resource mediated eco-friendly synthesis of zinc oxide nanoparticles and their photocatalytic application against dyes contaminated water, *Chem. Eng. J. Adv*., 16, 100536(2023). https://doi.org/10.1016/J.CEJA.2023.100536

Coll, S. C., Rubio, H. M., Ducrot, A., Norkute, E., Liu, X., Ebrahim, F. M., Smit, B., Thulstrup, P. W. and Hosta, R. L., A novel PEG-mediated approach to entrap hemoglobin (Hb) within ZIF-8 nanoparticles: Balancing crystalline structure, Hb content and functionality, *Biomater. Adv.,* 163, 213953(2024). https://doi.org/10.1016/J.BIOADV.2024.213953

De-Lucas, G. E., Leret, P., Monte, S. M., Reinosa, J. J., Enríquez, E., Del, C. A., Cañete, M., Menéndez, J., Fernández, J. F. and Rubio, M. F., ZnOnanoporous spheres with broad-spectrum antimicrobial activity by physicochemical interactions, *ACS Appl. Nano Mater.*, 1(7), 3214–3225(2018). https://doi.org/10.1021/ACSANM.8B00402

El-Boubbou, K., Lemine, O. M., Algessair, S., Madkhali, N., Al-Najar, B., AlMatri, E., Ali, R. and Henini, M., Preparation and characterization of various PVPylated divalent metal-doped ferrite nanoparticles for magnetic hyperthermia, *RSC Adv*., 14(22), 15664–15679(2024). https://doi.org/10.1039/D4RA01600A

Endeshaw, S. B., Goddati, M., Lee, J., Aga, F. G., Tufa, L. T. and Sabir, F. K., ZnO/CuOnanocomposites for enhanced photocatalytic and antibacterial applications: A comparative study of synthesis methods, *J. Sci. Adv. Mater. Dev*., 10(3), 100898(2025). https://doi.org/10.1016/J.JSAMD.2025.100898

Gurusamy, M., Sellavel, M. and Kuppuvelsamy, V. B., A sustainable green synthesis for photocatalytic and antibacterial activity of zinc oxide nanoparticles using Cucumismaderaspatanus leaf extract, *Desalin. Water Treat.,* 319, 100457(2024). https://doi.org/10.1016/J.DWT.2024.100457

Jailani, A., Hidzer, M. H., Firdaus, A. H. M., Sapuan, S. M., Zainudin, E. S., Atiqah, A., Wan Jaafar, W. M. and Suryanegara, L., Enhancing polyvinyl alcohol (PVA) nanocomposites: Key properties, applications and challenges in advanced engineering, *Defence Technol*., 01679(2025). https://doi.org/10.1016/J.DT.2025.05.020

Kaur, H., Sharma, A., Anand, K., Panday, A., Tagotra, S., Kakran, S., Singh, A. K., Alam, M. W., Kumar, S., Bouzid, G., Dalal, J. and Singh, G., Green synthesis of ZnO nanoparticles using E. cardamomum and zinc nitrate precursor: A dual-functional material for water purification and antibacterial applications, *RSC Adv*., 15(21), 16742–16765(2025). https://doi.org/10.1039/D5RA01469G

Khaleel, M. R., Hashim, F. S. and Alkhayatt, A. H. O., Impact of pH and ZnO NPs on the fabricated PVA-PVP/ZnOnanofibers: Morphology, absorption behavior, anticancer, and antibacterial activity, *Ceram. Int*., 50(20), 40161–40170(2024). https://doi.org/10.1016/J.CERAMINT.2024.07.283

Kumari, A., Sharma, D., Sharma, V. and Singh, B., Synthesis and characterization of sterculia gum-zwitterionicsulfobetaine-PVP based network hydrogels for biomedical application, *Hybrid Adv*., 8, 100341(2025). https://doi.org/10.1016/J.HYBADV.2024.100341

Lin, P. Y., Huang, Y. H., Chen, J. S., Sharma, R. K., Das, K., Sukul, U., Dey, G., Banerjee, P., Shinde, M., Taharia, M. and Chen, C. Y., Cost-effective microbial induced ZnO synthesis for building material: Antibacterial, photocatalytic and mechanical characteristics, *Environ. Technol. Innov*., 36, 103762(2024). https://doi.org/10.1016/J.ETI.2024.103762

Liu, Y., Liu, Y., Li, X., Qian, Y., Lv, L. and Wang, Y., Fabrication and research of $Mg(OH)_2$/PCL/PVP nanofiber membranes loaded by antibacterial and biosafe $Mg(OH)_2$ nanoparticles, *Polymer. Test*., 112, 107635(2022). https://doi.org/10.1016/J.POLYMERTESTING.2022.107635

Magar, M. H., Adole, V. A., Waghchaure, R. H. and Pawar, T. B., Efficient photocatalytic degradation of eosin blue dye and antibacterial study using nanostructured zinc oxide and nickel modified zinc oxide, *Res. Chem.,* 4, 100537(2022). https://doi.org/10.1016/J.RECHEM.2022.100537

Mezel, M., Alsous, M. B., Abbas, B., Aljoumaa, K., Assfour, B., Mousa, N. and Assaad, I., Multimode gradient-index fiber coated with a blend of PEG and PVP as a humidity sensor, *Res. Optics*., 16, 100697(2024). https://doi.org/10.1016/J.RIO.2024.100697

Nazir, A., Akbar, A., Baghdadi, H. B., urRehman, S., Al-Abbad, E., Fatima, M., Iqbal, M., Tamam, N., Alwadai, N. and Abbas, M., Zinc oxide nanoparticles fabrication using Eriobotrya japonica leaves extract: Photocatalytic performance and antibacterial activity evaluation, *Arabian J. Chem*., 14(8), 103251(2021). https://doi.org/10.1016/J.ARABJC.2021.103251

Nguyen, N. T. T., Phan, A. N. Q., Tran, T. V. and Nguyen, T. T. T., Antibacterial and photocatalytic activities of fruit-extract-mediated synthesized ZnO nanoparticles, *Nanoscale Adv*., 7(11), 3514–3527(2025). https://doi.org/10.1039/D5NA00211G

Nisha, J. A., Anilkumar, P. and Preetha, S., Eco-friendly fabrication of ZnOnanocomposites using Lepidium didymium and polymer-assisted CTAB/PEG: A multifunctional approach for enhanced biomedical applications, *J. Mol. Liq*., 417, 126550(2025). https://doi.org/10.1016/J.MOLLIQ.2024.126550

Panchami, H. R., Isloor, A. M., Vijesh, A. M. and Farnood, R., Innovative membrane engineering: Polyphenylsulfone/silver-doped zinc oxide for high-efficiency protein rejection, *Curr. Res. Green Sustain. Chem*., 10, 100460(2025). https://doi.org/10.1016/J.CRGSC.2025.100460

Prabhu, A., Lamani, A. R., Shetty, S. J., Bhat, S. S., Bhat, A. R., Jayanna, H. S. and Gurumurthy, S. C., Biosynthesis of ZnO nanoparticles using Averrhoabilimbi fruit extract: Evaluation of photocatalytic and antibacterial activities, *Inorg. Chem. Commun*., 180, 114989(2025). https://doi.org/10.1016/J.INOCHE.2025.114989

Raha, S. and Ahmaruzzaman, M., ZnO nanostructured materials and their potential applications: Progress, challenges and perspectives, *Nanoscale Adv*., 4(8), 1868–1925(2022). https://doi.org/10.1039/D1NA00880C

Rutherford, D., Bařinková, M. Š., Jamatia, T., Šuly, P., Cvek, M. and Rezek, B., Capping agent control over the physicochemical and antibacterial properties of ZnO nanoparticles, *Appl. Surf. Sci*., 692, 162739(2025). https://doi.org/10.1016/J.APSUSC.2025.162739

Sharma, R. K., Bandichhor, R., Mishra, V., Sharma, S., Yadav, S., Mehta, S., Arora, B., Rana, P., Dutta, S. and Solanki, K., Advanced metal oxide-based nanocatalysts for the oxidative synthesis of fine chemicals, *Mater. Adv.,* 4(8), 1795–1830(2023). https://doi.org/10.1039/D2MA00977C

Sheehab, N. T., Hashim, F. S., Al-Bermany, E., Obaid, A. N., Abdali, K. and Alkhayatt, A. H. O., Performance of TiO_2-SiC nanomaterials on morphology and sorption behavior of PVA-PEG-based nanocomposites for UV-applications and antibacterial efficacy, *Nano-Struct. Nano-Obj*., 42, 101479(2025). https://doi.org/10.1016/j.nanoso.2025.101479

Uzoeto, H. O., Nkiru, A., Aisida, S. O. and Ezema, F. I., Enhanced microstructural properties and biocompatibility of zinc oxide nanoparticles by biogenic synthesis protocol for antibacterial applications, *Hybrid Adv*., 7, 100332(2024). https://doi.org/10.1016/J.HYBADV.2024.100332

Villegas, F. A., Castellano, L. E., Vilchis, N. A. R., and Luque, P. A., Sustainable and environmentally friendly synthesis of ZnO semiconductor nanoparticles from Bauhinia forficata leaves extract and the study of their photocatalytic and antibacterial activity, *Cleaner Mater*., 13, 100268(2024). https://doi.org/10.1016/J.CLEMA.2024.100268